



Original Research Article

**$\gamma$ -Fe<sub>2</sub>O<sub>3</sub>@KSF: A recyclable catalyst for the efficient synthesis of pyrano-pyrimidinone derivatives**

Masoud Mohammadi Zeydi<sup>1,2\*</sup> and Masoumeh Sedighi Gildeh<sup>2</sup>

<sup>1</sup>Department of Organic Chemistry, University of Guilan, Rasht, Iran.

<sup>2</sup>Department of Chemistry, Tonekabon Branch, Islamic Azad University, Tonekabon, Iran

\*Corresponding author number: Tel.: +989395145655

\*E-mail: zedi.65@gmail.com

---

**ABSTRACT**

In this work,  $\gamma$ -Fe<sub>2</sub>O<sub>3</sub>@KSF as a stable heterogeneous and magnetic catalyst was prepared by the successive coating of  $\gamma$ -Fe<sub>2</sub>O<sub>3</sub> shell on KSF core. The prepared reagent was characterized using different methods including FT-IR, XRD, TGA and SEM techniques and used for the one-pot synthesis of pyrano-pyrimidinone derivatives. All reactions were performed under mild conditions, during short reaction times in high yields. The catalyst could be easily recovered by an external magnet and reused several times without any considerable loss of its activity.

**Keyword:**  $\gamma$ -Fe<sub>2</sub>O<sub>3</sub>@KSF, heterogeneous, magnetic, pyrano-pyrimidinone

---

## 1.Introduction

Performing organic reactions in the presence of heterogeneous catalysts are extraordinary important, but in most cases, one of major problems of this group of catalysts is their down activity. All nanoparticles (NPs) known as quasi-homogeneous catalysts are allocated between heterogeneous and homogeneous catalysts due to their extensive surface area and improved dispersal ability in most organic reactions [1]. Scientists in various field such biotechnology, as biomedicine, materials science, physics, and catalysis paired their attention to the magnetic nanoparticles. This attention can be attributed to their wide ratio of surface area to volume, behavior of the paramagnetic and low toxicity [2]. Nanoparticles often have the favorite specifications of both inorganic and organic catalysts [3]. Among these nanoparticles, iron oxides, magnetite ( $\text{Fe}_3\text{O}_4$ ) and maghemite ( $\gamma\text{-Fe}_2\text{O}_3$ ) because of a high saturation magnetization and their less toxicity than their metallic peers, and super paramagnetic behavior are excellent choice due to the biocompatibility of the magnetic nanoparticles [4, 5]. Some of unique feature of the MNPs as catalysts separated by magnetic forces, increase product's purity and have optimize operations [6]. Other advantage of this kind of separation is avoiding the use of dangerous chemicals and additional filtration during the separation process. Consequently, it is a green process. pyrano-pyrimidinones exists in a large number of compounds with pharmaceutical activity such as antitumor [7], antihypertensive [8], antibacterial activity [9], antileishmanial activity [10], and antipyretic, anti-inflammatory and gastroprotective properties [11]. Different methods using various catalysts were offered for the preparation of pyrano-pyrimidinones which of them L-proline [12], diammonium hydrogen phosphate [13], tetrabutylammonium bromide [14],  $\text{KAl}(\text{SO}_4)_2 \cdot 12\text{H}_2\text{O}$  (alum) [15], DABCO [16], Al-HMS-20 [17], succinimidinium hydrogensulfate ( $[\text{H. Suc}]\text{HSO}_4$ ) [18] sulfonic acid nanoporous silica (SBA-Pr- $\text{SO}_3\text{H}$ ) [19], Nano-sawdust- $\text{OSO}_3\text{H}$  [20], and ZnO-supported copper oxide [21] are examples. It is

noteworthy that, most of the proposed methods have disadvantages such as low yields, long reaction times, monotonous work-up, rough reaction conditions, and requirement of excess value of catalysts or reagents. As a result, it is very important to provide more suitable methods for the preparation of pharmaceutical compounds. To our knowledge, there has been very little report on the use of heterogeneous acid catalyst in water as environment solvent for the synthesis of pyrano-pyrimidinones. As a result of our continuous research plans on the preparation of pyrano-pyrimidinones, and in continuance of our previous works [22-30], we here reported condensation reaction of aromatic aldehyde **1** barbituric acid **2** with malononitrile **3** by using of  $\gamma$ -Fe<sub>2</sub>O<sub>3</sub>@KSF as heterogeneous acid catalyst for quickly prepared the pyrano[2,3-*d*]pyrimidinones (**4a-m**) in good yields (Scheme 2).

## 2. Experimental section

### 2.1. Material

All chemicals were procured from Merck and Aldrich companies. All reported yields refer to isolated products. The product structure was confirmed by comparing their physical characteristics, FT-IR and NMR spectroscopy with reliable samples and reported in the literature. Monitoring the progress of the reaction and determine the purity of the compounds were scouted by Thin-layer chromatography (TLC). Melting points were measured by Buchi B-545 apparatus, the FT-IR spectra were recorded with Perkin-Elmer spectrum BX series spectrophotometer. X-ray diffraction (XRD) measurements were performed by Siemens D-4500 X-ray diffract meter (Rigaku), using Cu K $\alpha$  radiation (1.5406 Å) at room temperature. Scanning electron microphotographs (SEM) were afforded on an SEM-Germany LEO 1430VP. Thermo gravimetric analyses (TGA) were afforded by Polymer Laboratories PL-TGA thermal analysis instrument. Catalyst was heated from 25 to 800 °C, at ramp 20 °C min<sup>-1</sup> under N<sub>2</sub> atmosphere.

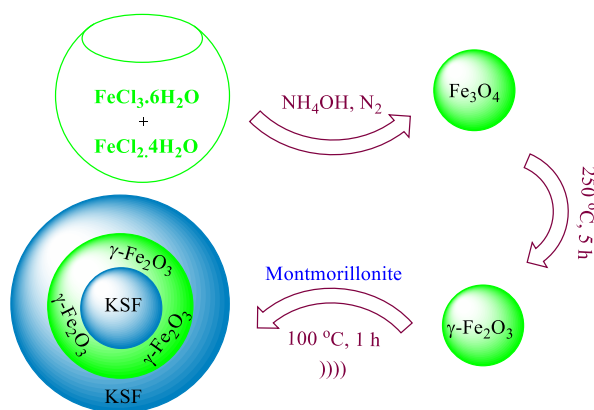
## 2.2. Synthesis of nanoparticles $\gamma$ -Fe<sub>2</sub>O<sub>3</sub>

The nanoparticles  $\gamma$ -Fe<sub>2</sub>O<sub>3</sub> was prepared by reported chemical technique [31]. FeCl<sub>3</sub>.6H<sub>2</sub>O (4.89 g) and FeCl<sub>2</sub>.4H<sub>2</sub>O (3 g) were dissolved in deionized water (50 mL) at room temperature and under Argon atmosphere. At the same temperature, NH<sub>4</sub>OH solution (0.6 M, 330 ml) was added drop wise to the stirring mixture to reach the reaction pH to 11. The black suspension was stirred for 1 hour at room temperature, and then it was stirred for 1 hour under reflux conditions to produce brown dispersion. Finally, the magnetic nanoparticles  $\gamma$ -Fe<sub>2</sub>O<sub>3</sub> were separated by an external magnet and washed with deionized water for several times. The collected sediment was heated for 5 hours at 250 °C to produce reddish-brown powder.

## 2.3. Synthesis of NPS $\gamma$ -Fe<sub>2</sub>O<sub>3</sub>@KSF

NPS  $\gamma$ -Fe<sub>2</sub>O<sub>3</sub>@KSF was prepared using the reported method [31] with a few modifications. The synthesized  $\gamma$ -Fe<sub>2</sub>O<sub>3</sub> (3.5g) was added to glacial acetic acid (30 mL), then montmorillonite (1.5g) in deionized water (100 mL) was added slowly under ultrasonic irradiation during 20 min and the mixture was kept at 100 °C for 1 hour under vigorous stirring. The nanoparticles of  $\gamma$ -Fe<sub>2</sub>O<sub>3</sub>@KSF were collected by an external magnet. Then, the precipitate was washed with deionized water and dried at 50 °C in vacuum for 12 h

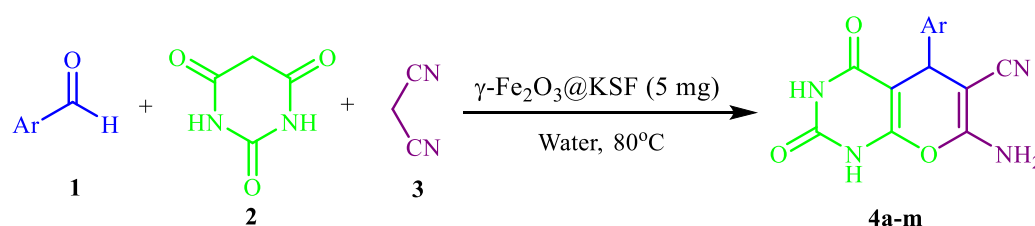
(Scheme1).



**Scheme 1.** Preparation of NPS  $\gamma$ -Fe<sub>2</sub>O<sub>3</sub>@KSF

## 2.4. General method for the synthesis of pyrano[2,3-*d*]pyrimidines

$\gamma$ -Fe<sub>2</sub>O<sub>3</sub>@KSF (5 mg) was added to a mixture of aromatic aldehyde (1 mmol), malononitrile (1.2 mmol), barbituric acid (1 mmol) and water (5 mL) in a 10 mL round-bottomed flask. The reaction mixture was stirred at 80 °C for an appropriate time (Table 2). The progress of the reaction was characterized using TLC [*n*-hexane:ethyl acetate (4:1)]. After completion of the reaction, the nano-catalyst was removed in the presence of an external magnet, water was evaporated and the desired product was purified by recrystallization in hot EtOH (Scheme 2).



**Scheme 2.** Synthesis of pyrano[2,3-*d*]pyrimidinones by  $\gamma$ -Fe<sub>2</sub>O<sub>3</sub>@KSF

## 2.5. Catalyst characterization

### 2.5.1. FT-IR analysis

Figure 1 displays the FT-IR spectra of  $\gamma$ -Fe<sub>2</sub>O<sub>3</sub> and  $\gamma$ -Fe<sub>2</sub>O<sub>3</sub>@KSF. Significant change in the wide band ranging from 480 cm<sup>-1</sup> to 1600 cm<sup>-1</sup> is detected in the FT-IR spectra of the  $\gamma$ -Fe<sub>2</sub>O<sub>3</sub>@KSF, which can be allocated to the overlapping peak between the KSF bridging stretching modes and Fe-O vibrations. The O-H bending bond modes observed peaks at about 1432 and 1520 cm<sup>-1</sup>. The broad peak at around 3400 cm<sup>-1</sup> and 1630 cm<sup>-1</sup> corresponds to the bending H-O-H bond vibration of water molecules that adsorb on the surface of  $\gamma$ -Fe<sub>2</sub>O<sub>3</sub>@KSF [32].

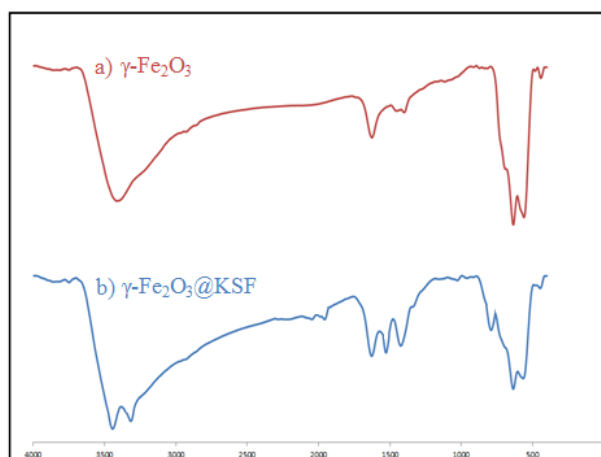


**Figure 1.** FT-IR spectra of nano  $\gamma\text{-Fe}_2\text{O}_3$  (a);  $\gamma\text{-Fe}_2\text{O}_3\text{@KSF}$  (b)

### 2.5.2. Powder X-ray diffraction

XRD chart of the  $\gamma\text{-Fe}_2\text{O}_3\text{@KSF}$  is shown in Figure 2. In this chart diffraction peaks from the  $\gamma\text{-Fe}_2\text{O}_3$  can be clearly seen ( $2\theta = 30.1^\circ, 35.5^\circ, 43.1^\circ, 53.5^\circ, 57.0^\circ$  and  $62.6^\circ$ ), marked by their indices (2 2 0), (3 1 1), (4 0 0), (4 2 2), (5 1 1) and (4 4 0) are observed. Moreover, five diffraction peaks are appeared at around ( $2\theta = 9.3^\circ, 16.8^\circ, 18.6^\circ, 20.1^\circ$  and  $27.3^\circ$ , which can be attributed to diffraction peaks of KSF. These results indicate that  $\gamma\text{-Fe}_2\text{O}_3$  nanoparticles are successfully installed on the surface of KSF [33].

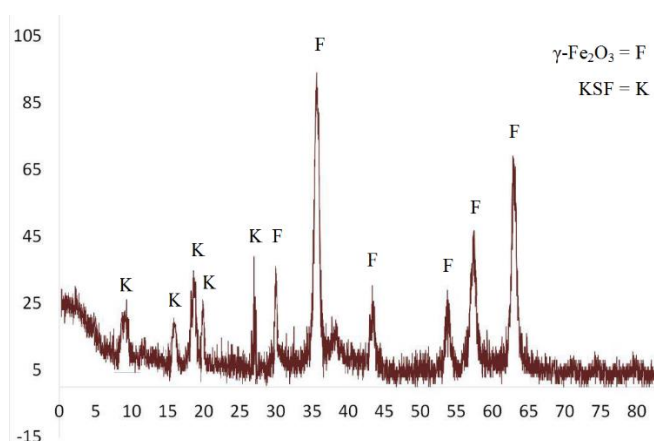


**Figure 2.** XRD patterns of  $\gamma\text{-Fe}_2\text{O}_3\text{@KSF}$  catalyst

### 2.5.3. SEM Analysis

Figure 3 show the SEM images of  $\gamma\text{-Fe}_2\text{O}_3\text{@KSF}$  which prepared by montmorillonite precursor at  $100^\circ\text{C}$ . An image shows that the newly formed  $\gamma\text{-Fe}_2\text{O}_3$  magnetic layers are

uniformly and porous coated onto the KSF core. As shown in Figure 4a, the external surface of  $\gamma\text{-Fe}_2\text{O}_3\text{@KSF}$  is rough. Moreover, from Figure 4b, it was found that the size of the  $\gamma\text{-Fe}_2\text{O}_3\text{@KSF}$  catalyst were around 38–44 nm.

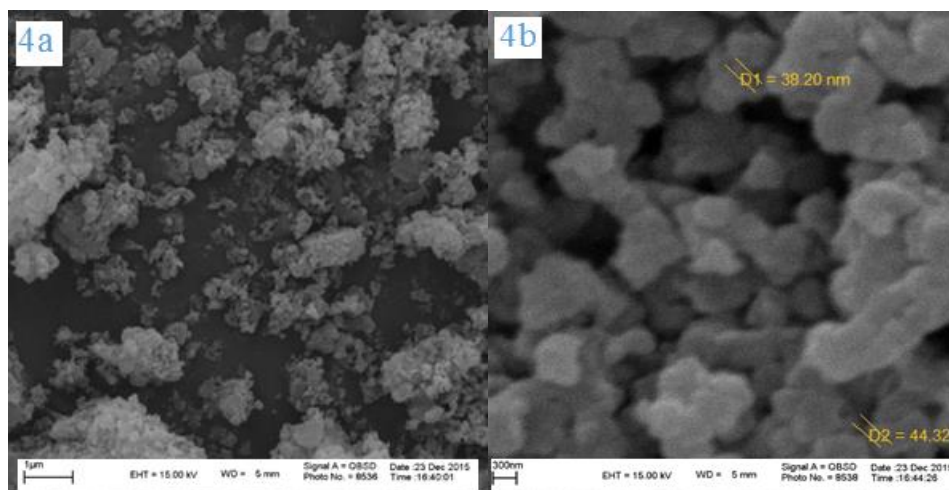


**Figure 3.** SEM images of  $\gamma\text{-Fe}_2\text{O}_3\text{@KSF}$  catalyst

#### 2.5.4. TGA Analysis

Figure 4 shows the TGA of the  $\gamma\text{-Fe}_2\text{O}_3\text{@KSF}$  sample, which in it the loss of about 5% of weight at 130°C can be related to the loss of surface absorbed water and the reduction of about 12% of weight up to 430°C is ascribed to the decomposition of part from the surface bond.

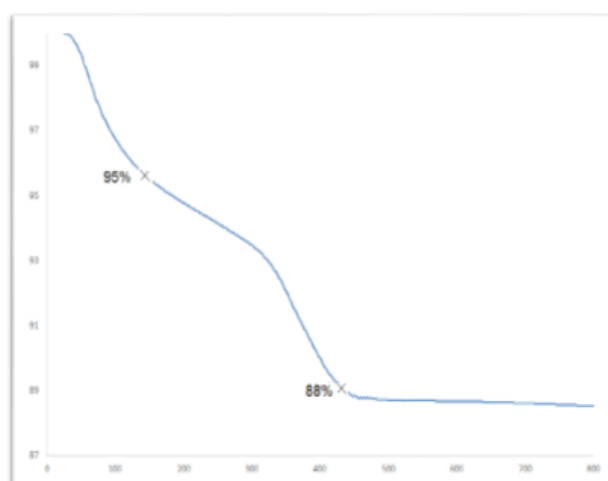


**Figure 4.** TGA curve of  $\gamma\text{-Fe}_2\text{O}_3\text{@KSF}$

### 3. Results and discussion

In the last decade, introduction of new nano catalysts for the advancement of chemical reactions became an important of our ongoing research program [28]. In continuation of these studies we were interested to investigate the preparation of a new magnetic nanocomposite  $\text{Fe}_2\text{O}_3@KSF$  and its applicability in the development of chemical reactions. So, here in we report the results obtained from the acceleration of the synthesis of pyrano[2,3-*d*]pyrimidinone derivatives using this reagent as the catalyst.

In a preliminary experiment the reaction of 4-chlorobenzaldehyde (1 mmol) with barbituric acid (1 mmol) and malononitrile (1.2 mmol) was studied in the presence of the prepared nano-catalyst  $\gamma\text{-Fe}_2\text{O}_3@KSF$ , as a model reaction. In this study different conditions, including use of various amounts of the catalyst, temperature and various solvents such as EtOH,  $\text{H}_2\text{O}$ , MeOH,  $\text{CH}_3\text{CN}$  and solvent-free conditions were examined and the results are summarized in (Table 1). On the basic of these studies it can be concluded that the best results can be obtained using 5 mg of the catalyst at 80 °C in water as the solvent (Table 1, entry 6). Using higher amounts of MNPs  $\gamma\text{-Fe}_2\text{O}_3@KSF$  did not affect the reaction yields.

**Table 1.** The effect of solvent, amount of the catalyst and temperature on the synthesis of pyrano[2,3-*d*]pyrimidinone derivatives in the presence of  $\gamma\text{-Fe}_2\text{O}_3@KSF$

Entry	Catalyst (mg)	Temp (°C)	Solvent	Time (min)	Yield (%) <sup>a</sup>
1	5	Reflux	$\text{CH}_3\text{CN}$	60	...
2	5	Reflux	MeOH	60	50
3	5	Reflux	EtOH	60	75
4	5	50	EtOH	60	60
5	5	Reflux	$\text{H}_2\text{O}$	4	94
6	5	80	$\text{H}_2\text{O}$	6	94
7	5	80	-	30	80
8	10	80	$\text{H}_2\text{O}$	4	90
9	15	80	$\text{H}_2\text{O}$	4	94

<sup>a</sup> Isolated yields

After optimization of reaction conditions and in order to explore the scope of this procedure, the  $\gamma$ -Fe<sub>2</sub>O<sub>3</sub>@KSF catalyst was used for the preparation of pyrano[2,3-*d*]pyrimidinone derivatives from various aldehydes, barbituric acid and malononitrile under the optimal reaction conditions. The obtained results showed that this conversion can also be occurred with high yields in short times (Table 2).

**Table 2.** Preparation of pyrano[2,3-*d*]pyrimidinone derivatives using Fe<sub>2</sub>O<sub>3</sub>@KSF catalyst.

Entry	products	Aldehyde	Time (min)	Yield (%) <sup>a</sup>	Mp (°C)	
					Found	Rep. [ref.]
1	4a	C <sub>6</sub> H <sub>5</sub> CHO	6	93	213-215	215-217[36]
2	4b	2-ClC <sub>6</sub> H <sub>4</sub> CHO	10	90	208-210	211-212[36]
3	4c	3-ClC <sub>6</sub> H <sub>4</sub> CHO	11	88	238-240	240-241[34]
4	4d	4-ClC <sub>6</sub> H <sub>4</sub> CHO	8	94	241-242	237-240[35]
5	4e	2-NO <sub>2</sub> C <sub>6</sub> H <sub>4</sub> CHO	8	90	253-255	253-255[35]
6	4f	3-NO <sub>2</sub> C <sub>6</sub> H <sub>4</sub> CHO	8	86	268-270	267-269[34]
7	4g	4-NO <sub>2</sub> C <sub>6</sub> H <sub>4</sub> CHO	8	89	234-235	236-238[37]
8	4h	4-MeOC <sub>6</sub> H <sub>4</sub> CHO	8	84	280-281	266-268[35]
9	4i	2-OHC <sub>6</sub> H <sub>4</sub> CHO	11	92	161-163	160-162[36]
10	4j	4-OHC <sub>6</sub> H <sub>4</sub> CHO	10	87	204-207	204-206[34]
11	4k	4-NMe <sub>2</sub> C <sub>6</sub> H <sub>4</sub> CHO	8	92	229-231	231-233[36]
12	4l	4-BrC <sub>6</sub> H <sub>4</sub> CHO	8	90	230-232	228-230[37]
13	4m	4-CH <sub>3</sub> C <sub>6</sub> H <sub>4</sub> CHO	10	86	226-228	225-227[36]

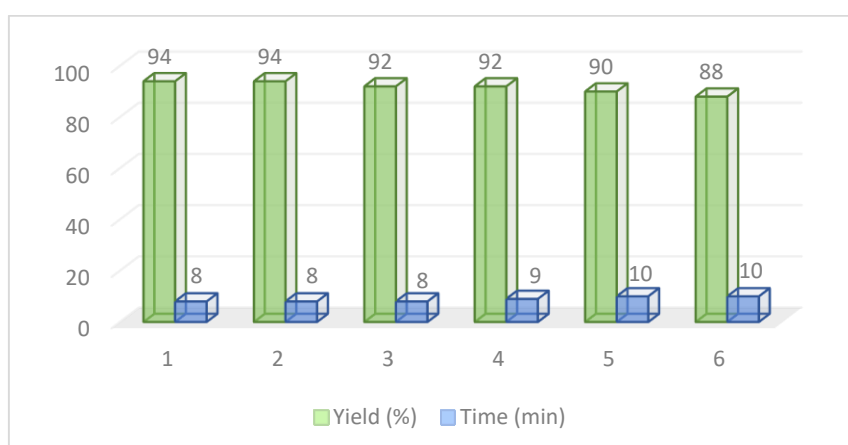
In order to show the suitability of this procedure the efficiency of nano catalyst  $\gamma$ -Fe<sub>2</sub>O<sub>3</sub>@KSF with the other catalysts in the preparation of 7-amino-6-cyano-5-(4-chlorophenyl)-5*H*-pyrano[2,3-*d*]pyrimidinone **4d** is compared in Table 3. As shown in this Table, the newly developed procedure avoids some of the disadvantages associated with the other methods such as high temperature, harsh reaction conditions, use of toxic or moisture sensitive catalyst, use of higher amounts of the catalysts and recoverability of the catalyst. On the basis of the included results we can say that  $\gamma$ -Fe<sub>2</sub>O<sub>3</sub>@KSF is efficient than the other referenced procedures.

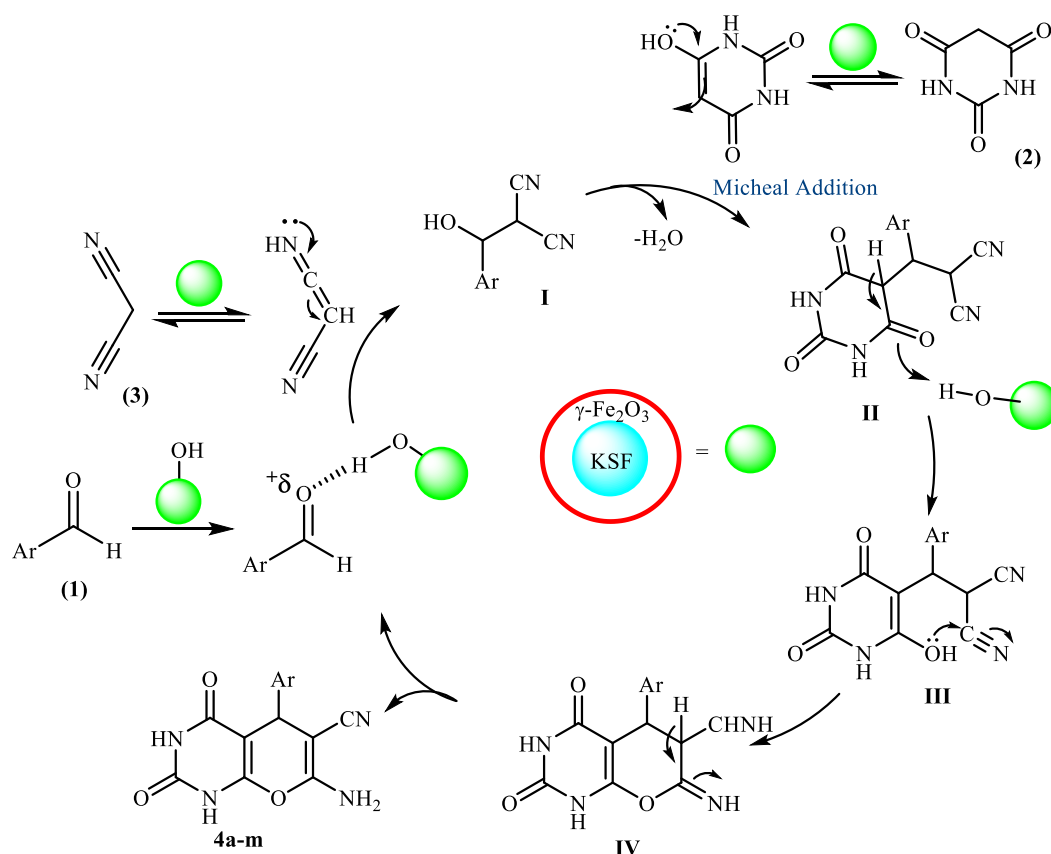
**Table 3.** Comparison of the results obtained from the synthesis of 7-amino-6-cyano-5-(4-chlorophenyl)-5*H*-pyrano[2,3-*d*]pyrimidinone **4d** in the presence of KSF@ $\gamma$ -Fe<sub>2</sub>O<sub>3</sub> with other catalysts.

Entry	Catalyst [ref.]	Conditions	Time (min)	Yield (%) <sup>a</sup>
1	<i>L</i> -proline (17 mol%) [12]	H <sub>2</sub> O: EtOH, r.t.	45	73
2	Tetrabutylammonium bromide (TBAB) (10 mol%) [14]	H <sub>2</sub> O, reflux	35	80
3	DABCO (10 mol%) [16]	H <sub>2</sub> O: EtOH, r.t.	120	92
4	Sulfonic acid nanoporous silica (SBA-Pr-SO <sub>3</sub> H) (0.02 g) [19]	Solvent-free, 140 °C	15	90
5	Nano-Sawdust-OSO <sub>3</sub> H (0.02 g) [20]	EtOH/reflux	15	92
6	CuO/ZnO nanocatalyst (0.03 g) [21]	H <sub>2</sub> O, reflux	10	92
7	Al-HMS-20 (0.03 g) [17]	EtOH, r.t	12 (h)	95
8	([SuSA-H]HSO <sub>4</sub> ) (0.05 mmol) [34]	H <sub>2</sub> O, 80 °C	8	92
9	[DABCO](SO <sub>3</sub> H) <sub>2</sub> Cl <sub>2</sub> [35]	H <sub>2</sub> O, reflux	25	83
10	$\gamma$ -Fe <sub>2</sub> O <sub>3</sub> @KSF (5 mg) <sup>b</sup>	Water, 80 °C	8	94

<sup>a</sup>Isolated yield.<sup>b</sup>This work.

Recycling of the catalysts are a key process in environmental concerns. Hence, after the completion of the reaction, to check the reusability of  $\gamma$ -Fe<sub>2</sub>O<sub>3</sub>@KSF, the nano particles were recovered by an external magnet, washed with ethanol several times and dried at 80 °C for 1 hour. The recovered nano catalyst successfully catalyzed the reaction between 4-chlorobenzaldehyde, barbituric acid and malononitrile under the optimized reaction conditions. This procedure was used at least for 6 runs without considerable change in the reaction time and yield (Figure 5).

**Figure 5.** Reusability of the  $\gamma$ -Fe<sub>2</sub>O<sub>3</sub>@KSF catalyst in the synthesis of pyrano[2,3-*d*]pyrimidinones derivative



**Scheme 3.** Proposed mechanism for the formation of pyrano[2,3-*d*]pyrimidinones using  $\gamma\text{-Fe}_2\text{O}_3\text{@KSF}$

A proposed mechanism for the formation of pyrano[2,3-*d*]pyrimidinones can be seen in Scheme 3. As claimed by this mechanism and in the first step, the aldehyde **1** is activated by the  $\gamma\text{-Fe}_2\text{O}_3\text{@KSF}$  catalyst. Then, the carbonyl carbon is attacked by the nucleophilic compound to produce the intermediate **I**. On the other way, the Micheal addition tautomerizes **2** in the presence of the nano catalyst  $\gamma\text{-Fe}_2\text{O}_3\text{@KSF}$  to generate intermediate **II**. Afterward, it cyclizes to give intermediate **III** which is tautomerizes to prepare the fully aromatized compound **4a-m** (Scheme 3).

#### 4. Conclusion

In summary, in this study, we have introduced  $\gamma\text{-Fe}_2\text{O}_3\text{@KSF}$  nanocomposite as a stable magnetic catalyst that it was synthesis by the successive coating of  $\gamma\text{-Fe}_2\text{O}_3$  shell on KSF core using a mixed solvent method. It was applied as a magnetically recyclable heterogeneous

nano catalyst for the preparation of pyrano[2,3-*d*] pyrimidinones derivatives from reaction of various aldehydes, barbituric acid and malononitrile in water. The practical procedure show some advantages including high yields, operational simplicity, no by-products, and easy work up due to no need to column chromatography for isolation, product separation and catalyst recycling are easy and simple with the assistance of an external magnet.

### Acknowledgments

We are thankful to the Research Council of the Islamic Azad University, Tonekabon Branch for partial support of this work.

### References

- [1] V. Polshettiwar, R. Luque, A. Fihri, H. B. Zhu, M. Bouhrara, J. M. Bassett, *Chem. Rev.*, 111, 3036 (2011).
- [2] A. H. Lu, E. L. Salabas, F. SchUth, *Angew. Chem. Int. Ed.*, 46, 1222 (2007).
- [3] R. Cano, D. J. Ramon, M. Yus, *Tetrahedron*, 67, 5432 (2011).
- [4] D. J. Widder, W. L. Greif, K. J. Widder, R. R. Edelman, T. J. Brady, *Am. J. Roentgenol.*, 148, 399 (1987).
- [5] A. R. Kiasat, S. Nazari, *J. Mol. Catal. A Chem.*, 365, 80 (2012).
- [6] Y. Xu, S. Huang, M. Xie, Y. Li, L. Jing, H. Xu, Q. Zhang, H. Li, *New. J. Chem.*, 40, 3413 (2016).
- [7] E. M. Grivsky, S. C. Lee, W. Sigel, D. S. Duch, C. A. Nichol, *J. Med. Chem.*, 23, 327 (1980).
- [8] L. R. Bennett, C. J. Blankely, R. W. Fleming, R. D. Smith, D. K. Tessonam, *J. Med. Chem.*, 24, 382 (1981).
- [9] R. B. Ajmal, S. D. Rajendra, S. S. Rupali, *Int. J. Pharma Biosci.*, 5, 422 (2014).
- [10] A. R. Agarwal, N. Ashutosh, P. M. S. Goyal, S. G. Chauhan, *Bioorg. Med. Chem.*, 24, 6678 (2005).

- [11] O. Bruno, S. Schenone, A. Ranise, E. Barocell, M. Chiavarini, V. Ballabeni, S. Bertoni. *Arzneim. Forsch.*, 50, 140 (2000).
- [12] M. Bararjanian, S. Balalaie, B. Movassagh, A. M. Amani. *J. Iran. Chem. Soc.*, 6, 436 (2009).
- [13] S. Balalaie, S. Abdolmohammadi, H. R. Bijanzadeh, A. M. Amani. *Mol. Divers.*, 12, 85 (2008).
- [14] A. Mobinikhaledi, M. A. B. Fard. *Acta Chim. Slov.*, 57, 931 (2010).
- [16] J. Azizian, A. Shameli, S. Balalaie, M. M. Ghanbari, S. Zomorodbakhsh, M. Entezari, S. Bagheri, G. Fakhrpour. *Orient. J. Chem.*, 28, 327 (2012).
- [17] B. Sabour, M. H. Peyrovi, M. Hajimohammadi. *Res. Chem. Intermed.*, 41, 1343 (2015).
- [18] O. Goli. Jolodar, F. Shirini, M. Seddighi. *J. Iran. Chem. Soc.*, 13, 457 (2016).
- [19] G. M. Ziarani, S. Faramarzi, Sh. Asadi, A. Badiei, R. Bazl, M. Amanlou. *DARU J. Pharm. Sci.*, 21, 3 (2013).
- [20] B. Sadeghi, M. Bouslik, M. R. Shishehbore. *J. Iran. Chem. Soc.*, 12, 1801 (2015).
- [21] J. Albadi, A. Mansournezhad, T. Sadeghi. *Res. Chem. Intermed.*, 41, 8317 (2015).
- [22] N. O. Mahmoodi, M. Mohammadi Zeydi, E. Biazar, *J. Sulfur Chem.*, 37, 613 (2016).
- [23] M. Mohammadi Zeydi, S. Ahmadi, *Orient. J. Chem.*, 32, 2215 (2016).
- [24] N. O. Mahmoodi, M. Mohammadi Zeydi, E. Biazar, Z. Kazeminejad. *Phosphorus Sulfur Silicon Relat. Elem.*, 192, 344 (2016).
- [25] M. Mohammadi Zeydi, N. O. Mahmoodi, *Int. J. Nano. Dimens.*, 7, 174 (2016).
- [26] M. Mohammadi Zeydi, N. Montazeri, M. Fouladi, *J. Heterocycl. Chem.*, 54, 3549 (2017).
- [27] N. O. Mahmoodi, M. Mohammadi Zeydi, M. Mamaghani, N. Montazeri, *Res. Chem. Intermed.*, 43, 2641 (2017).

- [28] N. O. Mahmoodi, Z. Khazaei, M. Mohammadi Zeydi, *J. Iran. Chem. Soc.*, 14, 1889 (2017).
- [29] M. Mohammadi Zeydi, N. O. Mahmoodi, *J. Chin. Chem. Soc.*, 64, 1023 (2017).
- [30] M. Mohammadi Zeydi, N. O. Mahmoodi, M. Fouladi, M. Shamsi-Sani, *Iran. Chem. Commun.*, 6, 65 (2018).
- [31] Q. He, Z. Zhang, J. Xiong, Y. Xiong, H. Xiao, *Opt. Mater.*, 31, 380 (2008).
- [32] Y. Zhang, X. Yu, Y. Jia, Z. Jin, J. Liu, X. Huang, *Eur. J. Inorg. Chem.*, 33, 5096 (2011).
- [33] S. W. Lee, J. Drwiega, C. Y. Wu, D. Mazyck, W. M. Sigmund, *Chem. Mater.*, 16, 1160 (2004).
- [34] M. Vosooghi, S. Farzipour, M. Saeedi, N. Babazadeh, S. M. Mahdavi, S. Mahernia, A. Foroumadi, M. Amanlou, A. Shafie, *J. Iran. Chem. Soc.*, 12, 1487 (2015).
- [35] S. Sobhani, Z. Mesbah Falatoni, M. Honarmand, *RSC. Adv.*, 4, 15797 (2014).
- [36] F. Shirini, M. Safarpour Nikoo Langarudi, M. Seddighi, O. Goli Jolodar, *Res. Chem. Intermed.*, 41, 8483 (2015).
- [37] Y. Hu, J. Chen, Z.G. Le, Q.G. Zheng, *Synth. Commun.*, 35, 739 (2005).